Scientific Reports

https://doi.org/10.1038/s41598-026-38206-2

Article in Press

Investigation of the cutting effects on high-temperature granite based on cerchar abrasivity test

Received: 13 October 2025

Accepted: 29 January 2026

Published online: 14 March 2026

Cite this article as: Yang Q., Zhang H., Rui X. *et al.* Investigation of the cutting effects on high-temperature granite based on cerchar abrasivity test. *Sci Rep* (2026). https://doi.org/10.1038/s41598-026-38206-2

Qingshuai Yang, Hongwei Zhang, Xusheng Rui, Tianhua Yang & Ximin Song

Investigation of the cutting effects on high-temperature granite based on Cerchar abrasivity test

Xusheng Rui[1], Hongwei Zhang[1]*, Qingshuai Yang[1], Tianhua Yang[1], Ximin Song[1].

1.Key Laboratory of Disaster Prevention and Disposal in Coal Mining, Ministry of Emergency Management, China University of Mining and Technology(Beijing)

*Correspondence: Hongwei Zhang, China University of Mining and Technology (Beijing), Beijing 100083, China.

Email: hongwei@cumtb.edu.cn.

Data Availability

Not applicable

Author contributions

All authors contributed to the study conception and design. Material preparation, data collection and analysis were performed by Hongwei Zhang, Qingshuai Yang and Xusheng Rui. The first draft of the manuscript was written by Qingshuai Yang and all authors commented on previous versions of the manuscript. All authors read and approved the final manuscript.

Abstract

The high-temperature rock drilling is a key process in the exploitation of the hot-dry-rock (HDR) geothermal energy. Understanding the abrasive characteristics of HDR is critical for drilling efficiency and cost. Therefore, this study investigates the wear mechanism and cutting/scratch evolutions of granite under temperatures from 25°C to 500°C by using the Cerchar abrasive test. The results show that: (1) The Cerchar Abrasivity Index (CAI) of granite decreases with the increasing temperature and three characteristic decreasing stages can be found. (2) The CAI of granite and the average cutting force exerted on its surface during sliding exhibit a similar trend as temperature increases, the high temperature treatment reduces the cutting force during sliding. (3) Observing the scratches, it is found that the cutting force increases sharply and aggravates the wear of the steel stylus when the steel stylus encounters minerals with higher hardness such as quartz or biotite. (4) There is a significant negative correlation between the instantaneous cutting force and the scratch depth during sliding. In other words, the higher the instantaneous cutting force, the smaller the scratch depth, and high temperature treatment can reduce the penetration depth of the steel stylus. These data and laws provide important reference for HDR geothermal development and drilling processes to improve drilling efficiency and reduce development costs.

Keywords: Cerchar abrasive index; Cutting force; Scratch depth; High-temperature treatment; Geothermal drilling

Deep hot-dry-rock (HDR), a kind of high-temperature rock buried at depths more than 3 km with temperatures over 150°C and a high-quality geothermal resource. It has attracted widespread attention from different countries in the world due to its numerous advantages such as cleanliness, renewability, extensive reserves, widespread distribution, and favorable thermal continuity[1]. HDR is characterized by its low permeability, high temperature, and hardness. It requires hydraulic fracture stimulation to create or enhance fracture networks to increase the rock's permeability, forming an enhanced geothermal system (EGS).EGS involve drilling multiple injection and production wells and drilling through deep, hard, high-temperature HDR is essential to establish communication with underground geothermal reservoirs, enabling

effective heat exchange. Due to the need for advanced technology, specialized equipment and time, geothermal drilling represents one of the major technical and cost challenges in geothermal energy development[2]. A significant portion of the costs is attributed to drill bits wear (Fig. 1) which is driven by the deep, hard, and high-temperature conditions of HDR. These extreme conditions accelerate drill bit degradation, requiring frequent replacements and significantly contributing to the overall expenses of geothermal projects.

In order to improve drilling efficiency and reduce drilling costs, it is necessary to monitor different physical and mechanical parameters during drilling, such as the cutting force exerted on the drill bit, temperature, speed, etc. These data are essential to identify key issues during drilling, such as excessive bit wear or low drilling efficiency, and enable operators to promptly adjust drilling parameters such as bit type, hardness of drill bit and rotational speed. This proactive approach helps minimize the cost of deep hot dry rock drilling, extend the life of drilling equipment and increase drilling efficiency[3]. The abrasive characteristics of rocks are typically assessed through the Cerchar abrasive test, and different Cerchar Abrasivity Index (CAI) values are used to determine drill bit wear during the drilling process[4], and lower CAI value indicates less drill bit wear[5]. The magnitude of CAI value is not only dependent on the strength of the rock[6], but also on factors such as its stress state[4], composition[7], component proportions and distribution[8].

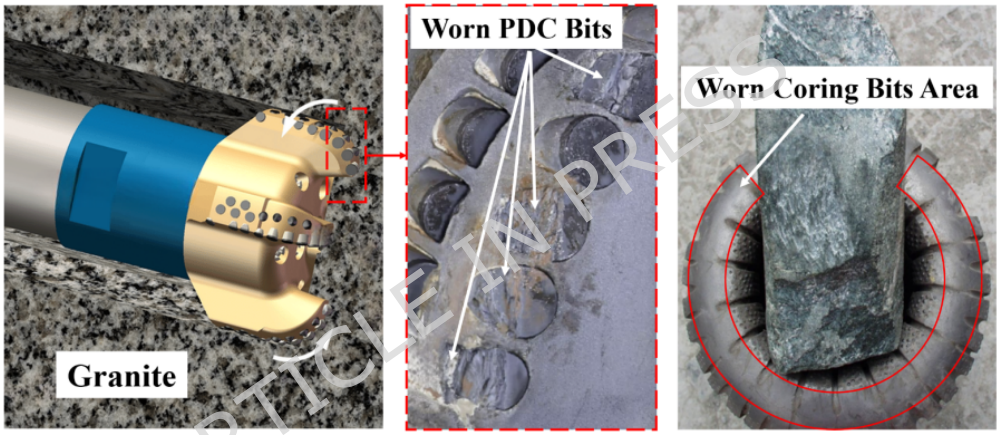

Fig. 1 Geothermal bit drilling wear and granite surface after drilling

Various studies on CAI of drill bits have been conducted in different institutes all of the world. Wang[9] indicated that the ISRM test standard's recommended 10 mm scratching distance remains suitable for thermally treated rock. Ji[5]found that the CAI value of Bukit Timah granite decreases with increasing temperature up to 600°C. Kahraman[10] concluded that the CAI of igneous rocks generally decreases as surface temperature and microwave energy increase. Bakar[11] calculate the CAI values for Garam Chashma Pluton and Kafiristan Pluton granites generally decrease when the temperature rises up to 500 °C, but increase due to the α–β quartz crystal transition at 600°C. However, there is limited research relating the abrasivity coefficient to key drilling parameters such as CAI, cutting force, drilling speed, and tool wear.

This study aims to investigate the variations in the abrasiveness of deep granite formations under different temperature conditions (up to 500°C) and their impact on key physical parameters during drilling operations. Specifically, the research will focus on analyzing the cutting forces exerted on the granite surface and the scratch depth of the drill bit under different thermal conditions. By combining data analysis with electron microscope observations of the scratches, this study will explore potential relationships among these variables at both the micro and macro levels, as well as the effects of high-temperature treatment. The findings

will provide theoretical insights for enhancing geothermal drilling engineering applications.

Rock Samples Preparation

The experimental sample is Luhui granite from Shandong province, China. The Luhui granite is gray white in color, gray black on the polished surface. It exhibits a fine-grained texture and a dense structure and has excellent resistance to acidic and alkaline environments. Table 1 illustrates the results of X-ray diffraction component analysis of Luhui granite with a density of 2.71×10^3kg/m^3. To minimize the discreteness in experimental data and to obtain consistent patterns of mechanical parameter variations, the same homogeneous and complete rock was selected for the test. The granite was divided into 6 cubes with side lengths of 50 mm, resulting in six experimental groups (Fig 2). The first group kept at ambient temperature (25°C) served as the control, and the remaining five groups of granite are heated to 100°C, 200°C, 300°C, 400°C, and 500°C respectively by using a muffle furnace at a heating rate of 2°C/min. After the sample is heated to the target temperature, it is kept in a muffle furnace for 2 hours and then naturally cooled to ambient temperature (Fig 3).

Table 1 Luhui granite X-ray diffraction component analysis

Sample No.	Temperature(℃)	Percentage(%)		
		Quartz	K-Feldspar	Feldspar
25-1	20	33.0	32.0	35.0
100-1	100	32.5	28.0	39.5
200-1	200	33.0	24.0	43.0
300-1	300	32.0	23.0	45.0
400-1	400	33.0	20.0	47.0
500-1	500	43.0	19.0	38.0

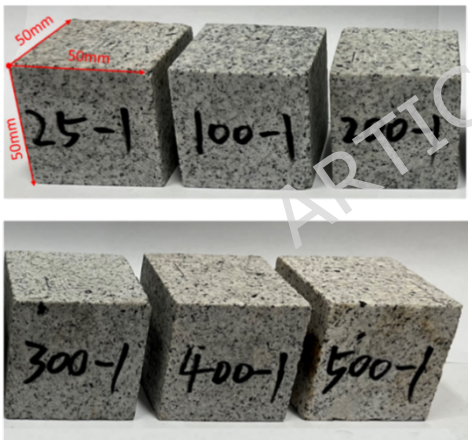

Fig. 2 Rock sample preparation

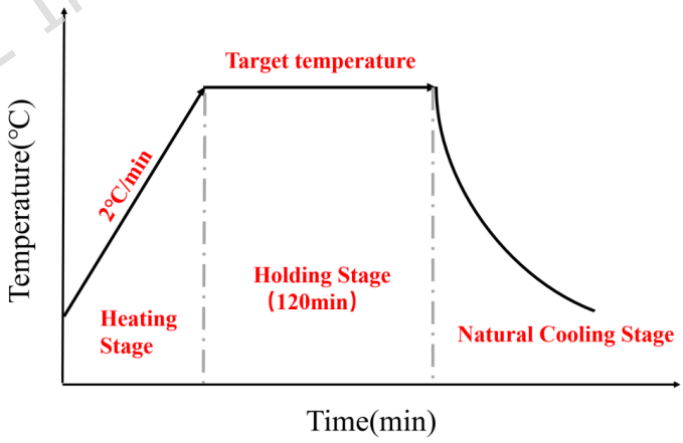

Fig. 3 Temperature vs time for granite samples heated in muffle furnace

CAI Experimental Equipment

The entire abrasive testing device is composed of a loading platform, propulsion device, pressure sensor, displacement sensor and a 70 N load. On the right side of the loading platform, a sample holder is equipped to secure the rock samples, ensuring their stability during the abrasion test. The upper loading platform is fitted with a freely vertically movable steel stylus. To comply with the standards prescribed by the International Society for Rock Mechanics (ISRM), a 70 N load is placed on the stylus to exert the required force during testing. A pressure sensor (Fig. 4a) is mounted on the left of the rock sample to measure the cutting forces exerted

on the rock sample by the steel stylus when sliding accurately in real time. A displacement sensor (Fig. 4b) is installed above the stylus to monitor the axial displacement of the stylus throughout the sliding process, aiding in analyzing changes in the scratch depth as it penetrates into the granite sample. The steel stylus used in the experiment measures 75 mm in length and 6 mm in diameter, with a tip angle of 90 degrees (Fig. 4c) and a Mohs hardness of 55[12].

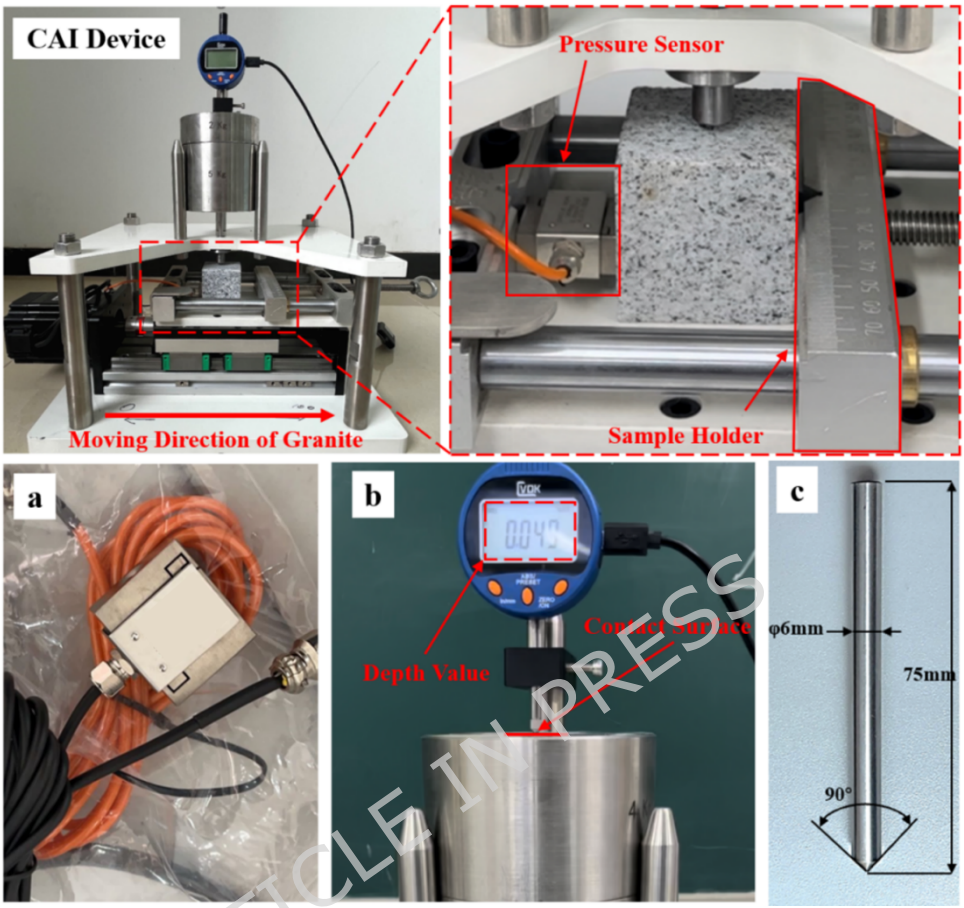

Fig. 4 Cerchar abrasivity testing device and key elements

The traditional CAI testing equipment is always employed to obtain the CAI value to evaluate the final wear state of the cutting tool or steel stylus. We implement a multi-sensor monitoring method to simultaneously measure the cutting force exerted on granite surface and scratch depth of stylus at the rock-steel interface during sliding. Additionally, the drive mechanism is computer-controlled to ensure consistent sliding speeds throughout the experiment and reduce experimental errors. This method provides valuable insights into the abrasive mechanisms and cutting responses of high-temperature HDR.

Cerchar Abrasivity Test

The rock sample was clamped by the holder device and the steel stylus was gently brought into contact with the surface of the rock sample from the upper slot, while a 70N load was placed above the steel stylus (Fig. 5). Set the sliding speed of the rock sample on the computer to 0.167 mm/s, allowing the steel stylus to move uniformly over 10 mm in 1 minute. This procedure was repeated five times on the same rock sample, with a different steel stylus used for each test, and data on the lateral shear force and vertical displacement of the stylus were collected concurrently during each sliding process.

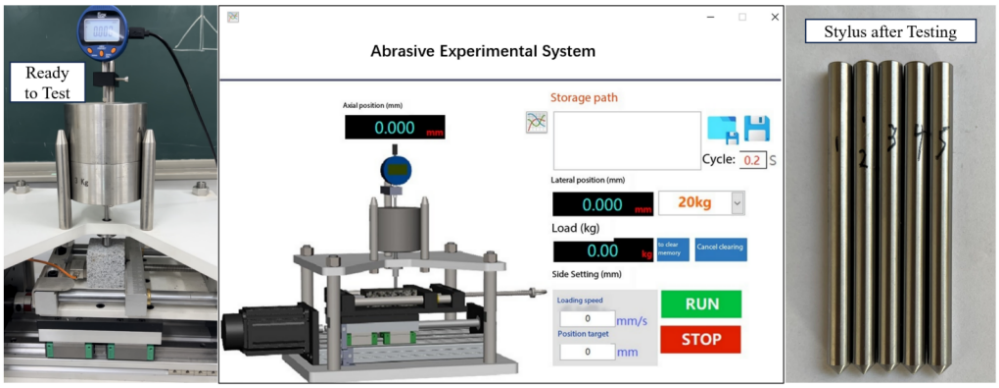

Fig. 5 Abrasive testing setup and results for steel stylus on rock sample

CAI value variation

When the steel stylus makes contact and slides against a granite sample, the friction results in the formation of a wear zone with planar characteristics at the stylus tip. After the removal of rock debris from the stylus end, it is positioned horizontally under an electron microscope for analysis. The associated measurement software is utilized to determine the diameter d of the erosion plane at the stylus tip, as shown in Fig 6. The stylus undergoes four measurements, with a rotation of 90 degrees between each[6]. Following these measurements, the Cerchar Abrasivity Index (CAI) is calculated using the method described in formula (1)[13]:

$$CAI = d \times 10 \quad (1)$$

where d is measured to an accuracy of 0.01 millimeters as the wear length at the tip of the stylus.

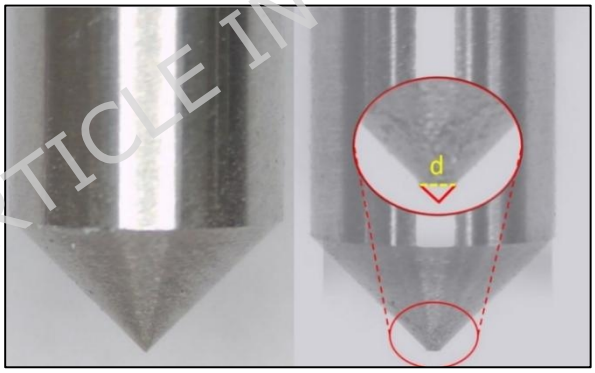

Fig. 6 Wear on tip of steel stylus before and after experimentation

Table 2 presents the results of the Cerchar abrasivity tests conducted on granite at 25°C. Fig 7 depicts the variation in granite abrasivity with temperature, indicating a general decline in CAI values as temperature increases. The average CAI value decreases markedly from 3.38 at ambient temperature to 2.74 at 100°C. It exhibits fluctuations within the range of 200°C to 400°C, with recorded values of 2.765, 2.745, and 2.796, respectively. The CAI value subsequently drops to 2.55 at 500°C.

Table 2 Cerchar abrasivity testing results with five test replications at 25℃

Test No.	1	2	3	4	5
Pin Hardness(HRC)	55	55	55	55	55
Measurement d_1(mm)	0.34	0.39	0.33	0.42	0.3
Measurement d_2(mm)	0.31	0.32	0.32	0.33	0.27
Measurement d_3(mm)	0.36	0.37	0.36	0.36	0.27
Measurement d_4(mm)	0.39	0.39	0.31	0.32	0.3
Mean reading d_M(mm)	0.35	0.37	0.33	0.36	0.29

Mean pin wear(mm)	0.34
CAI	3.4
Standard deviation of CAI	0.43

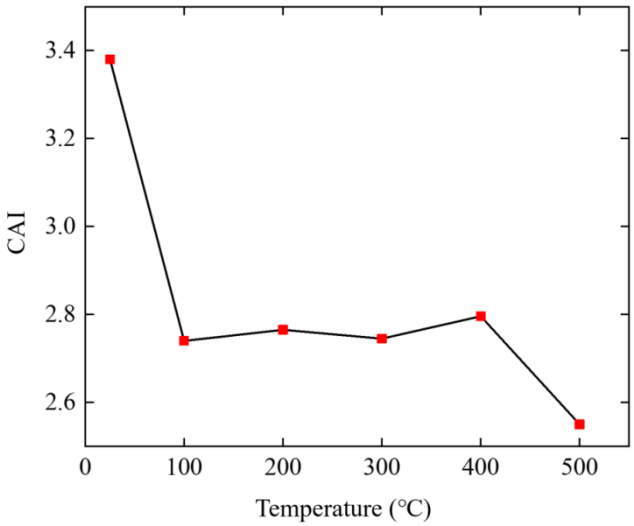

Fig. 7 CAI variation with increasing treatment temperature

Granite has high abrasion resistance without high-temperature treatment, which will cause increased wear on the drill bit. The CAI value depends largely on the presence of abrasive mineral content in the rock, the hardness and compressive strength of the rock sample[14,15]. The CAI decreases by 19.1% when temperatures rise from 25°C to 100°C, a change likely attributable to the evaporation of moisture within the granite. This moisture loss results in the formation of numerous pores and micro-cracks, which reduce the direct contact area between minerals such as quartz and feldspar and the steel stylus tip, thus diminishing the abrasion of the steel stylus. The most substantial thermal fracturing of granite occurs between 400°C and 500°C, characterized by the rapid development of micro-cracks and the emergence of a mylonite grain structure at 500°C[16]. This phenomenon is the primary factor behind the reduction in CAI values observed between 400°C and 500°C.[17]

Relationship between cutting force exerted on granite surface and CAI of granite with increasing temperature

We monitored the resistance and vertical displacement of the steel stylus during its sliding process by employing a pressure sensor positioned on the left side of the sample and a displacement sensor mounted above the stylus. The pressure sensor captured the resistance trend of the stylus, which reflects the cutting force exerted during sliding, as shown in Fig. 8. Similarly, the displacement sensor measured the vertical displacement, quantifying the scratch depth in the granite sample.

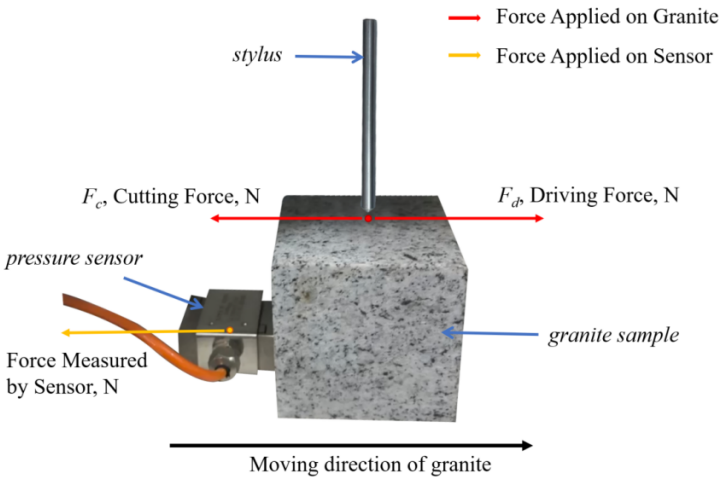

Fig. 8 Diagram to illustrate cutting force measurement via sensors on the left of granite

The average cutting force is defined as the mean force exerted by the granite surface on the steel stylus during the experiment, representing the overall frictional interaction between the two materials. Throughout the experiment, a series of discrete cutting force data points were collected using the pressure sensor. To compute the average cutting force, the sum of the cutting force values at all sampling points was divided by the total number of these points. The calculation is represented by the following formula:

$$F_{avg} = \frac{\sum_{i-1}^{n} F_i}{n}$$

where F_{avg} is the average cutting force, F_i is the cutting force at the i-th sampling point, and n represents the total number of sampling points.

The relationship between drill bit wear and cutting force is multifaceted. Typically, the application of cutting force leads to material wear and deformation, particularly evident as significant wear and shape changes at the tip of the drill bits. The magnitude of the force can often indicate the varying degrees of wear[18]. By comparing and analyzing the data of average cutting forces and CAI values collected at different temperatures, we have clarified the relationship between cutting force and wear in heat-treated granite. Additionally, this analysis has elucidated the reasons for variations in cutting force from microscopic perspective.

Fig. 9 illustrates the variation in average cutting force with increasing treatment temperature. Initially, the average cutting force was 190.6 N at 25°C. Upon heating to 100°C, it dropped sharply to 70.1 N and then fluctuated, reaching 83.2 N, 81.7 N, 117.3 N, and 71.9 N at 200°C, 300°C, 400°C, and 500°C, respectively. An anomalous increase in average cutting force was observed between 300°C and 400°C, which may be attributed to experimental errors and significantly deviates from the trend in CAI values. Overall, the trend in average cutting forces generally aligns with changes in the CAI with temperature. At ambient temperature, both the CAI and cutting forces reach their peak, indicating that steel stylus experiences maximum resistance under these conditions. As temperature rises to 500°C, both CAI and cutting forces show a decline. This trend can be attributed to the thermally induced formation and expansion of microcracks within the rock matrix. These microstructural changes compromise the rock's integrity, thereby diminishing its ability to withstand mechanical stress. Consequently, the rock becomes more susceptible to penetration and fragmentation during mechanical interactions, leading to reduced CAI values and cutting forces[7,19].

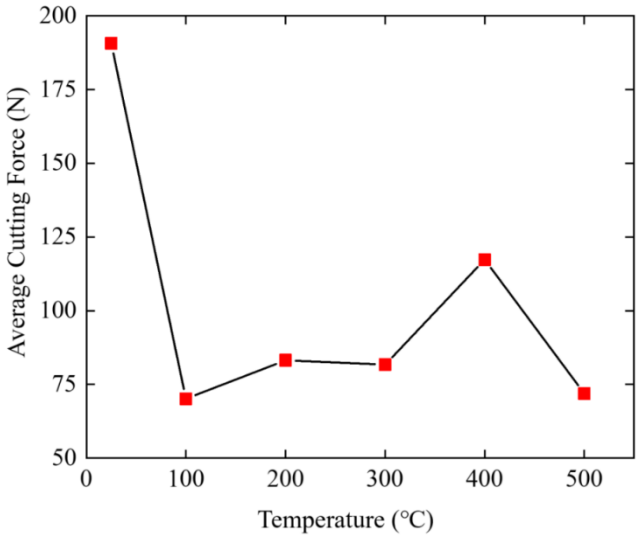

Fig. 9 Average cutting force variation with increasing treatment temperature

Observations of the peak cutting forces exerted by the steel stylus during its sliding motion revealed a significant increase in frictional resistance when encountering regions containing quartz (Fig. 10a) or biotite (Fig. 10b). This increase is notably correlated with the mineral hardness within the granite matrix. Particles worn off the stylus were found adhered to quartz, exhibiting a silver appearance, while biotite was visibly scratched by the stylus. The experimental steel stylus possesses a Mohs hardness of 5.5, which is lower than that of quartz and feldspar, recorded at 7 and 6, respectively[13]. Consequently, when the stylus encounters harder crystalline substances such as feldspar and quartz during its sliding motion, it fails to penetrate these material surfaces directly. This results in greater resistance and a rapid increase in cutting force, leading to significant wear at the tip of the stylus. [20,212223]

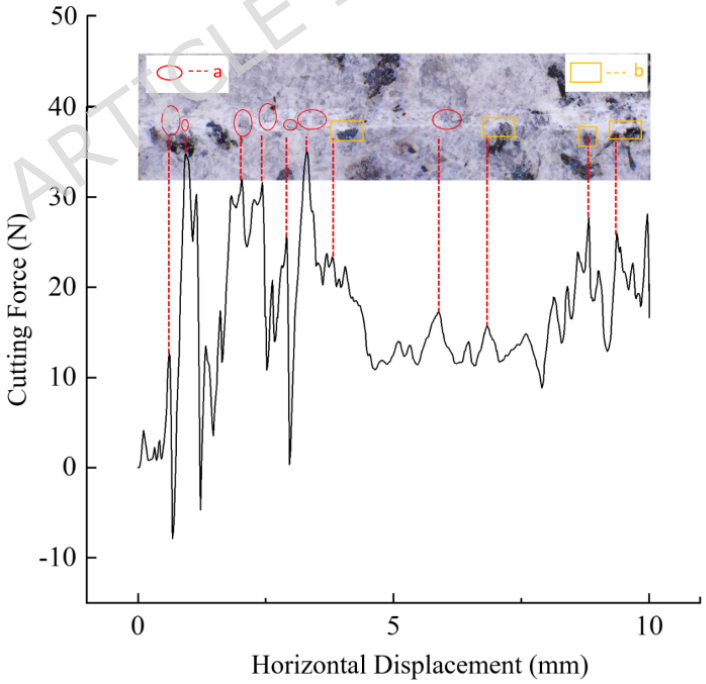

Fig. 10 Microscopic analysis of rock scratching: influence of quartz (a) and biotite (b) on peak cutting force

Variation of scratch depth with increasing temperature

The scratch depth is significantly influenced by the hardness of the rock; specifically, the harder the rock, the shallower the scratch depth[24], and conversely, softer rocks result in deeper

scratches. Typically, the frictional resistance encountered by the stylus increases with the penetration depth of the steel stylus, due to the enlargement of the effective cutting area at ambient temperature[25].

The average scratch depth refers to the mean depth to which the steel stylus penetrates the granite surface and enters into the rock during the experiment, reflecting the difficulty of the steel stylus embedding into the granite surface. Penetration depth data were collected at various temperatures using a displacement sensor, and by calculating the average, we can determine the average scratch depth on granite samples at each temperature. The calculation is represented by the following formula:

$$D_{avg} = \frac{\sum_{i-1}^{n} D_i}{n}$$

where D_{avg} is the average scratch depth, D_i is the scratch depth at the i-th sampling point, and n represents the total number of sampling points.

To analyze the average scratch depth of the steel stylus on granite samples at various temperatures, it was observed that the maximum depth, which is 0.122 mm, occurs at ambient temperature. There was a consistent decrease in scratch depth with increasing temperature, measuring 0.113 mm, 0.093 mm, 0.041 mm, 0.038 mm, and 0.067 mm at 100°C, 200°C, 300°C, 400°C, and 500°C, respectively (Fig. 11). This reduction can be attributed to moisture loss and the thermal expansion effects, which cause the mineral particles within the granite to compress and densify within the temperature range from room temperature to 300°C, resulting in increased rock strength and a significant decrease in scratch depth[26]. Between 400°C and 500°C, the formation of boundary cracks[15] leads to the softening of the rock, which consequently increases the scratch depth. Additionally, the reduced contact area between the stylus tip and the granite surface leads to a decrease in cutting force as the scratch depth decreases, consistent with the results from cutting force tests. Fig. 12 depicts the scratches on granite at 100°C and 400°C. It is evident that the scratches are more pronounced at 100°C, where the lighter color indicates the deeper, unoxidized mineral components of the granite.

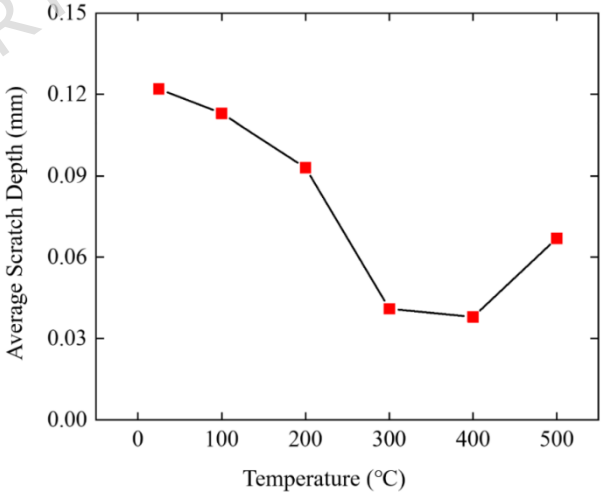

Fig. 11 Variation of average scratch depth with increasing treatment temperature

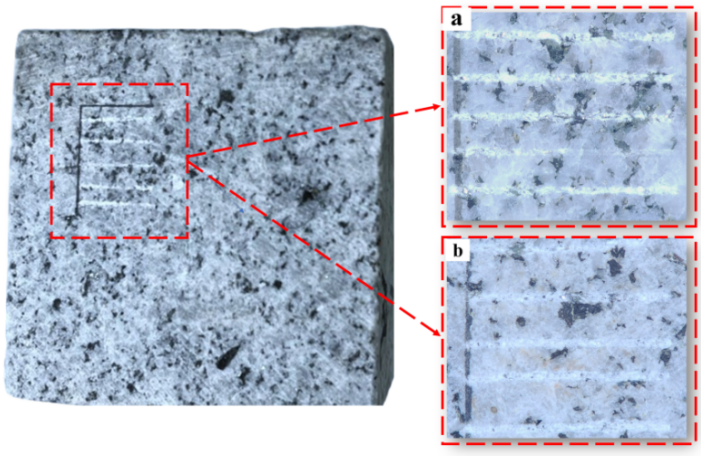

Fig. 12 Granite scratches at 100℃(a) and 400°C(b)

Relationship between cutting force exerted on granite surface and scratch depth of steel stylus

To investigate the relationship between instantaneous cutting forces and penetration depths during the sliding motion of the steel stylus at various temperatures, this study analyzed the correlation between cutting forces and scratch depth changes across 30 scratch tests using IBM SPSS Statistics. Bivariate Pearson correlation tests were conducted to calculate the correlation coefficient r and the P-value, determining the relationship between these variables. The bivariate Pearson correlation test, a widely utilized statistical technique, evaluates the linear association between two variables. This test quantifies the relationship using the correlation coefficient r, ranging from -1 to 1, where 1 indicates a perfect positive correlation, -1 a perfect negative correlation, and 0 no linear correlation. The significance of the correlation is assessed through a P-value, with values less than 0.05 generally considered statistically significant.

The data revealed a significant negative correlation between cutting force and scratch depth across the 30 sets. Specifically, as the cutting force exerted on the steel stylus significantly increased, the scratch depth notably decreased, and vice versa. For instance, the correlation between the cutting force and the scratch depth of the fifth scratch at 500°C was significantly negative. Due to the hardness of minerals such as quartz and feldspar, which exceeds that of the steel stylus, the friction resistance increases sharply when the stylus slides into these minerals. These hard minerals are difficult to cut, resulting in significant wear of the stylus and a corresponding decrease in penetration depth. This relationship is visually represented in Fig. 13, where the peaks of the cutting force correspond to the troughs of the scratch depth. In this context, the deeper penetration of the stylus is indicated by the descending trend of the scratch depth curve, illustrating that the maximum cutting forces coincide with the minimum scratch depths.

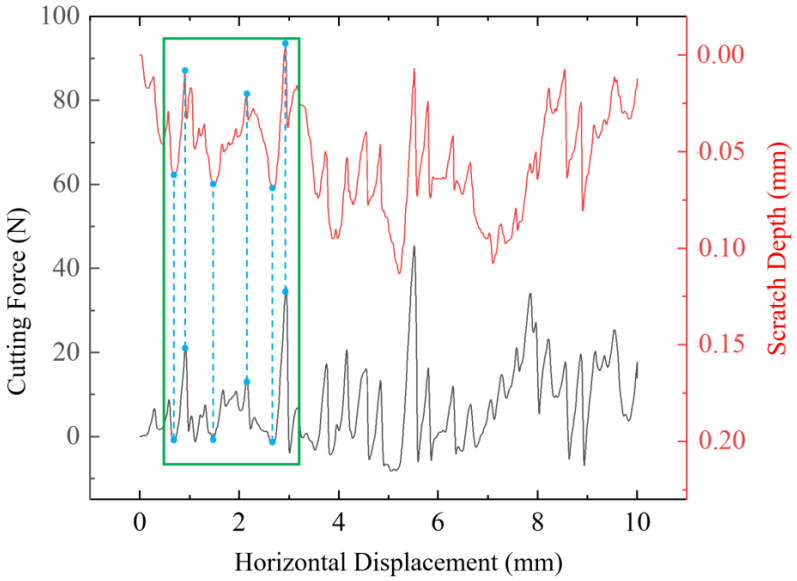

Fig. 13 Graph of cutting force and scratch depth variation with horizontal displacement

Conclusion

This study investigated the abrasion characteristics and physical properties of Luhui granite, using Cerchar abrasivity tests under various temperature treatments up to 500°C. The following conclusions could be drawn from the present study:

(1) With increasing temperatures, particularly in the intervals from 25°C to 100°C and 400°C to 500°C, there was a notable decrease in both the abrasiveness index of granite and the average cutting force exerted by the steel needle. This decrease was attributed to an increase in microfractures and changes in the granular structure of the granite. These two parameters exhibited similar trends throughout the entire temperature range.

(2) Scratch depth of stylus initially decreased and then increased as temperatures rose, influenced by thermal expansion effects and the formation of boundary cracks. A significant negative correlation was observed between the peak values of average cutting force and average scratch depth.

(3) The experimental results suggest that within a high-temperature dry heat environment below 500°C, thermally induced micro-fractures can effectively reduce drill bit wear, and the abrasiveness of deep high-temperature rocks can preliminarily be assessed through the average cutting force exerted on the drill bit.

The relationship between cutting force, scratch depth, and wear is extremely complex and influenced by multiple factors. This study primarily explored the interactions among these elements from a temperature perspective, yet microscopic-scale investigations were confined to observations via an electron microscope. Future research should consider additional parameters such as confining pressure and a broader range of temperatures, and employ various microscopic observation techniques, such as Scanning Electron Microscopy (SEM), to further validate these findings and provide a more comprehensive and in-depth understanding of the drilling processes in geothermal resource exploration.

References

1 Lv, T., Zhu, Q.-c., Lu, H.-b. & Li, X.-g. in *2009 International Conference on Energy and Environment Technology.* 683-686 (IEEE).

2 Rohit, R. *et al.* Tracing the evolution and charting the future of geothermal energy research and development. *Renewable and Sustainable Energy Reviews* **184**, 113531

(2023).

3 Capik, M. & Yilmaz, A. O. Correlation between Cerchar abrasivity index, rock properties, and drill bit lifetime. *Arabian Journal of Geosciences* **10**, 15 (2017).

4 Rostami, J., Ghasemi, A., Alavi Gharahbagh, E., Dogruoz, C. & Dahl, F. Study of dominant factors affecting Cerchar abrasivity index. *Rock mechanics and rock engineering* **47**, 1905-1919 (2014).

5 Ji, Y., Wang, L., Zheng, Y. & Wu, W. Temperature-dependent abrasivity of Bukit Timah granite and implications for drill bit wear in thermo-mechanical drilling. *Acta Geotechnica* **16**, 885-893 (2021).

6 Deliormanlı, A. H. Cerchar abrasivity index (CAI) and its relation to strength and abrasion test methods for marble stones. *Construction and Building Materials* **30**, 16-21 (2012).

7 Plinninger, R., Kaesling, H., Thuro, K. & Spaun, G. Testing conditions and geomechanical properties influencing the CERCHAR abrasiveness index (CAI) value. *International journal of rock mechanics and mining sciences* **40**, 259-263 (2003).

8 Capik, M. & Yilmaz, A. O. Development models for the drill bit lifetime prediction and bit wear types. *International Journal of Rock Mechanics and Mining Sciences* **139**, 104633 (2021).

9 Wang, L., Guo, K. & Wu, W. Abrasivity measurement of brittle rock after thermal treatment. *Measurement* **212**, 112710 (2023).

10 Kahraman, S., Saygin, E. & Fener, M. The effect of microwave treatment on the abrasivity of igneous rocks. *Arabian Journal of Geosciences* **17**, 21 (2024).

11 Abu Bakar, M., Ali, H. & Majeed, Y. Effects of heat treatment and confining pressure on rock abrasivity and its ramifications for bit wear and drillability in deep geothermal reservoirs. *Rock Mechanics and Rock Engineering* **56**, 8191-8208 (2023).

12 Suana, M. & Peters, T. The Cerchar abrasivity index and its relation to rock mineralogy and petrography. *Rock mechanics* **15**, 1-8 (1982).

13 Alber, M. *et al.* in *The ISRM suggested methods for rock characterization, testing and monitoring: 2007-2014* 101-106 (Springer, 2014).

14 Al-Ameen, S. & Waller, M. The influence of rock strength and abrasive mineral content on the Cerchar Abrasive Index. *Engineering Geology* **36**, 293-301 (1994).

15 Yin, T., Li, X., Cao, W. & Xia, K. Effects of thermal treatment on tensile strength of Laurentian granite using Brazilian test. *Rock Mechanics and Rock Engineering* **48**, 2213-2223 (2015).

16 Zhao, Y., Wan, Z., Feng, Z., Xu, Z. & Liang, W. Evolution of mechanical properties of granite at high temperature and high pressure. *Geomechanics and Geophysics for Geo-Energy and Geo-Resources* **3**, 199-210 (2017).

17 Mo, C., Zhao, J. & Zhang, D. Real-time measurement of mechanical behavior of granite during heating–cooling cycle: a mineralogical perspective. *Rock Mechanics and Rock Engineering* **55**, 4403-4422 (2022).

18 Rostamsowlat, I. Effect of cutting tool properties and depth of cut in rock cutting: an experimental study. *Rock Mechanics and Rock Engineering* **51**, 1715-1728 (2018).

19 Jeong, H., Choi, S. & Lee, Y.-K. Evaluation of cutting performance of a TBM disc cutter and Cerchar abrasivity index based on the brittleness and properties of rock. *Applied Sciences* **13**, 2612 (2023).

20 Li, M. *et al.* Effects of thermal treatment on the dynamic mechanical properties of coal measures sandstone. *Rock Mechanics and Rock Engineering* **49**, 3525-3539 (2016).

21 Yang, S.-Q., Ranjith, P., Jing, H.-W., Tian, W.-L. & Ju, Y. An experimental investigation on thermal damage and failure mechanical behavior of granite after exposure to different high temperature treatments. *Geothermics* **65**, 180-197 (2017).

22 Wong, L. N. Y., Zhang, Y. & Wu, Z. Rock strengthening or weakening upon heating in the mild temperature range? *Engineering Geology* **272**, 105619 (2020).

23 Zhang, F. *et al.* Nanoindentation tests on granite after heat treatment. *Rock Soil Mech.* **39**, - (2018).

24 Kolawole, O. & Ispas, I. Evaluation of geomechanical properties via scratch tests: where are we and where do we go from here? *SN Applied Sciences* **2**, 1633 (2020).

25 Thakur, M., Choudhary, B. S. & Seervi, V. An investigation into the effect of rock properties on drill bit life. *Journal of The Institution of Engineers (India): Series D* **105**, 655-664 (2024).

26 Huang, Y.-H. *et al.* Physical and mechanical behavior of granite containing pre-existing holes after high temperature treatment. *Archives of Civil and Mechanical Engineering* **17**, 912-925 (2017).

Acknowledgments

This study is supported by the Natural Science Foundation of Beijing, China (Grant No. 3232026), the National Natural Science Foundation of China (Grant No 52204162.), the Fundamental Research Funds for the Central Universities (Grant 2025ZKPYNY03), and the Education Foundation Of China University Of Mining & Technology-Beijing“ Fluidized mining of deep solid coal resources” (Grant XD2021018). The authors would also like to thank the journal editor and anonymous reviewers for their valuable suggestions.

Funding

Natural Science Foundation of Beijing, China (Grant No. 3232026), the National Natural Science Foundation of China (Grant No 52204162.), the Fundamental Research Funds for the Central Universities (Grant 2025ZKPYNY03), the Education Foundation Of China University Of Mining & Technology-Beijing" Fluidized mining of deep solid coal resources" (Grant XD2021018).

Author information

1.Key Laboratory of Disaster Prevention and Disposal in Coal Mining, Ministry of Emergency Management, China University of Mining and Technology(Beijing)

Xusheng Rui1, Hongwei Zhang1*, Qingshuai Yang1, Tianhua Yang1, Ximin Song1.

Author contributions

Xvsheng Rui: Writing - Original Draft and Validation, Hongwei Zhang: Review & Editing, Qingshuai Yang: Formal analysis, Tianhua Yang: Investigation.

Data availability statement

The authors will supply the relevant data in response to reasonable requests, if someone wants to request the data from this study, Please contact rxsping@163.com.

Ethics declarations

The authors declare no competing interests

Additional Information

1) The authors declare that there are no conflict of interests, we do not have any possible conflicts of interest.
2) The authors declare no conflict of interest, We declare that we have no conflict of interest.
3) The authors do not have any possible conflicts of interest.
4) The authors declare that they have no known competing financial interests or personal relationships that could have appeared to influence the work reported in this paper.

Figure legends

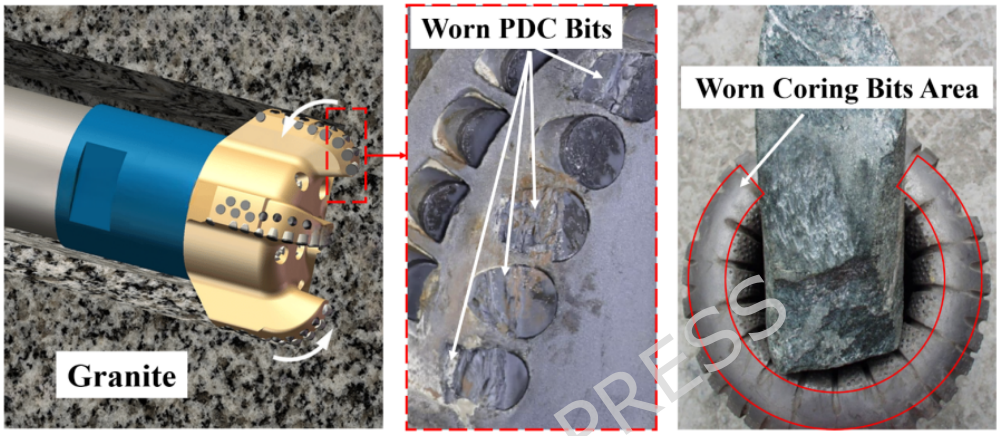

Fig. 1 Geothermal bit drilling wear and granite surface after drilling

Here, the wear state of PDC bits after cutting and drilling in high-temperature rock and the surface morphology of granite after drilling are cited in the field drilling of geothermal development projects to show the wear of PDC bits in field working conditions.

Fig. 2 Rock sample preparation

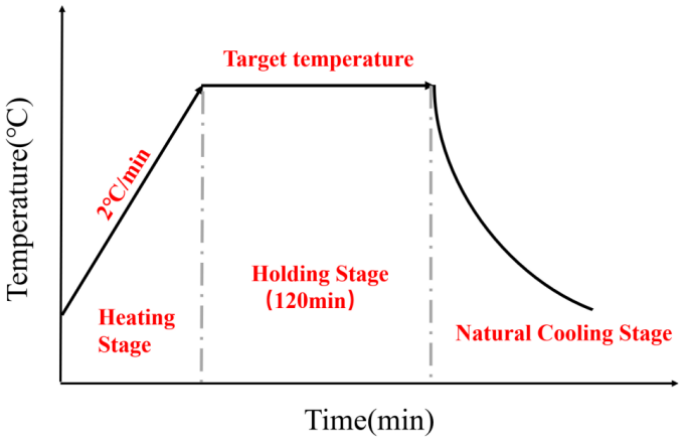

Fig. 3 Temperature vs time for granite samples heated in muffle furnace

The Lu grey granite specimen selected for this experiment was subjected to a natural cooling treatment after being heated in a muffle furnace at different temperatures. The specimen's surface morphology is shown in Fig. It can be seen that the specimen's surface colour changes significantly with increasing treatment temperature.

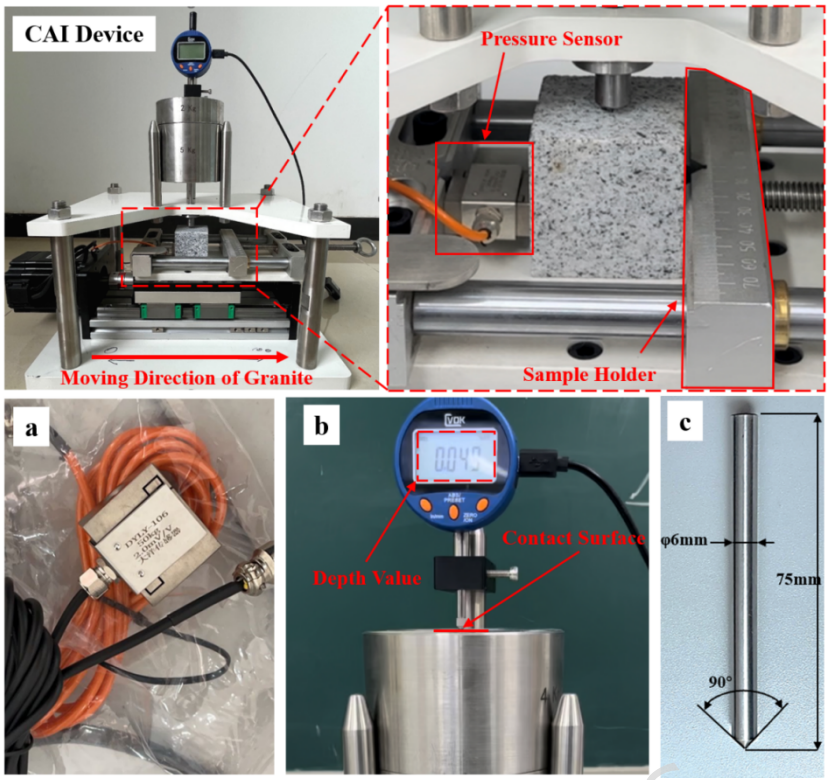

Fig. 4 Cerchar abrasivity testing device and key elements

The structure of the Cerchar abrasivity device is explained in detail here, with the specific components annotated as shown in the figure.

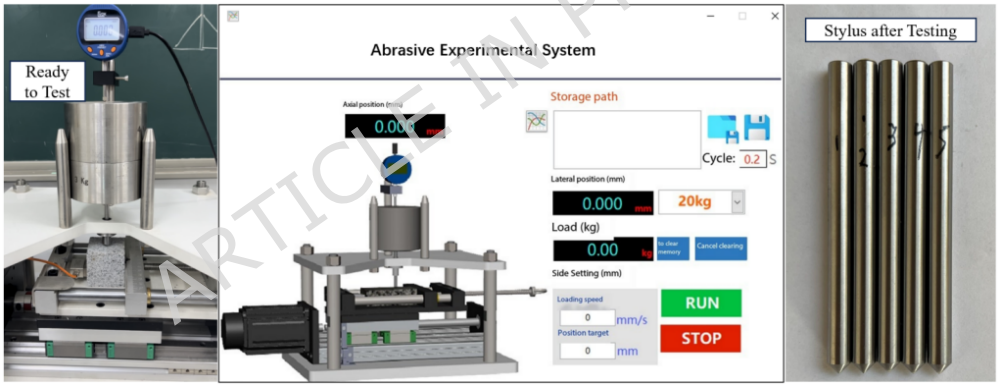

Fig. 5 Abrasive testing setup and results for steel stylus on rock sample

The rock sample was clamped by the holder device and the steel stylus was gently brought into contact with the surface of the rock sample from the upper slot, while a 70N load was placed above the steel stylus.

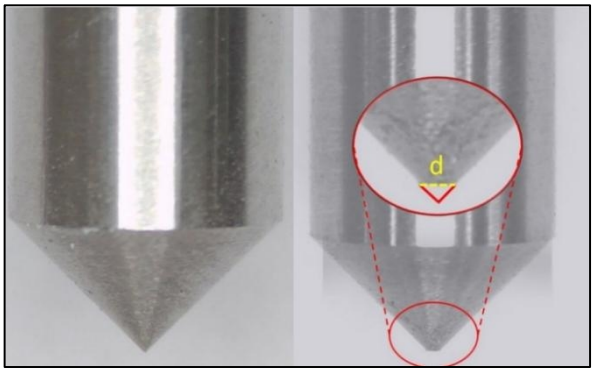

Fig. 6 Wear on tip of steel stylus before and after experimentation

The associated measurement software is utilized to determine the diameter d of the erosion

plane at the stylus tip, as shown in Fig 6.

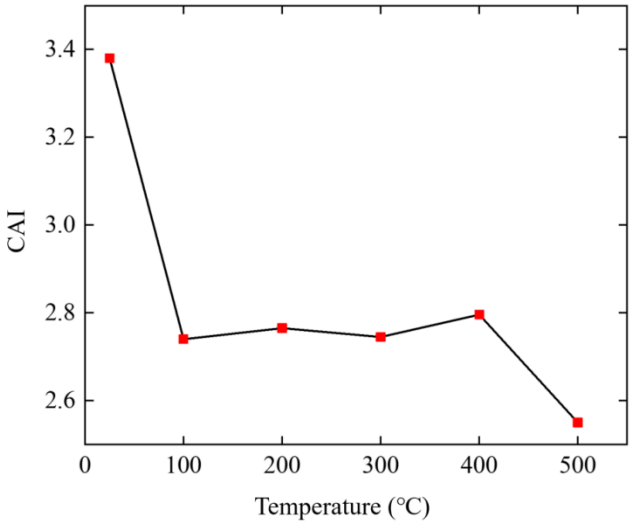

Fig. 7 CAI variation with increasing treatment temperature

Temperature effects on measured CAI values after heating and cooling treatments at different temperatures.

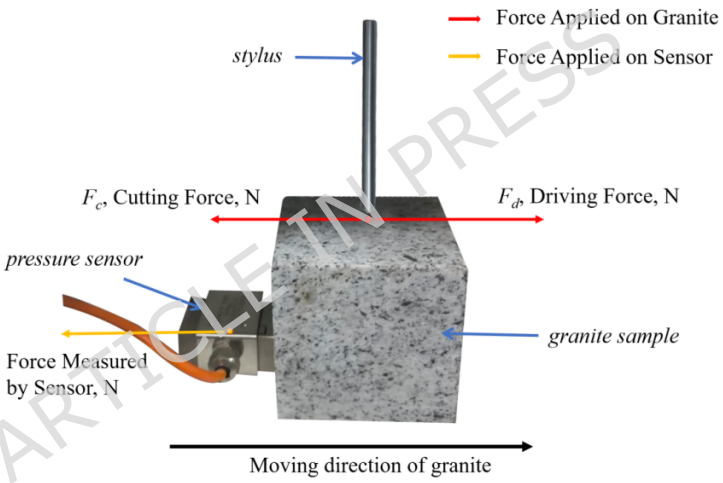

Fig. 8 Diagram to illustrate cutting force measurement via sensors on the left of granite

We monitored the resistance and vertical displacement of the steel stylus during its sliding process by employing a pressure sensor positioned on the left side of the sample and a displacement sensor mounted above the stylus.

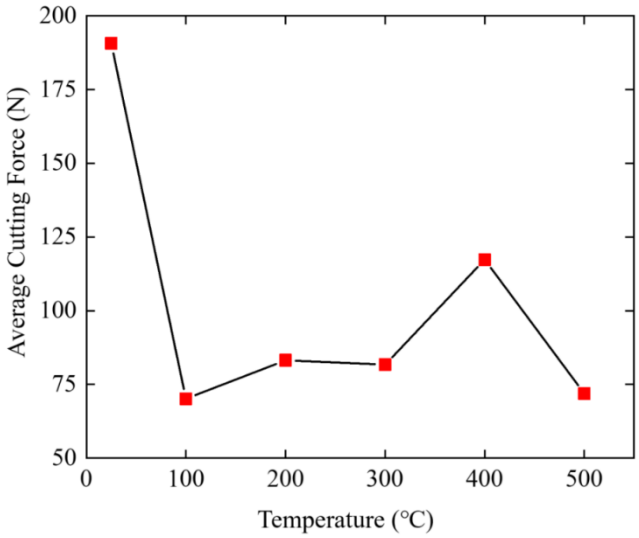

Fig. 9 Average cutting force variation with increasing treatment temperature

Temperature effects on measured average cutting force after heating and cooling treatments at different temperatures.

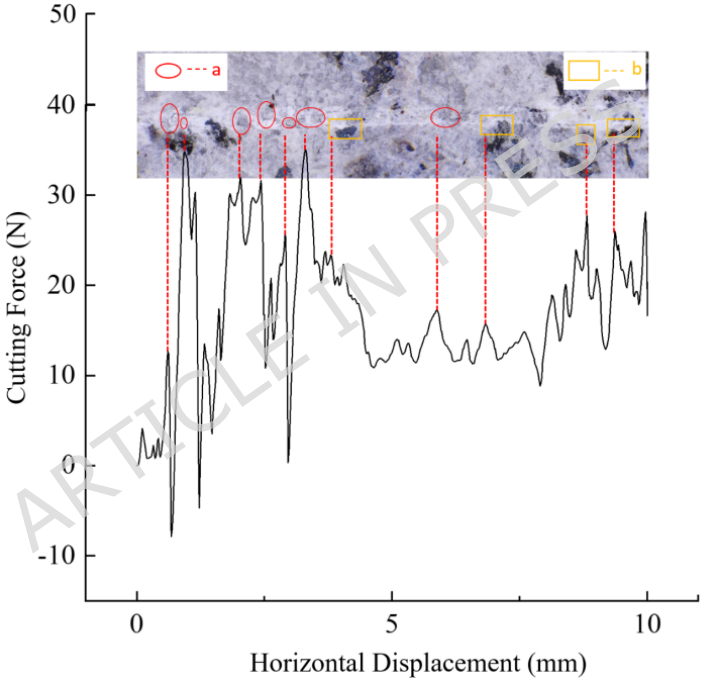

Fig. 10 Microscopic analysis of rock scratching: influence of quartz (a) and biotite (b) on peak cutting force

Differential horizontal displacement of steel stylus over different mineral grains during sliding.

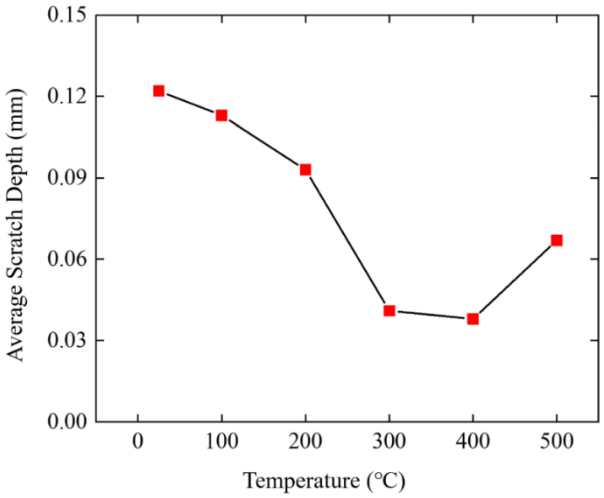

Fig. 11 Variation of average scratch depth with increasing treatment temperature

Temperature effects on measured average scratch depth after heating and cooling treatments at different temperatures.

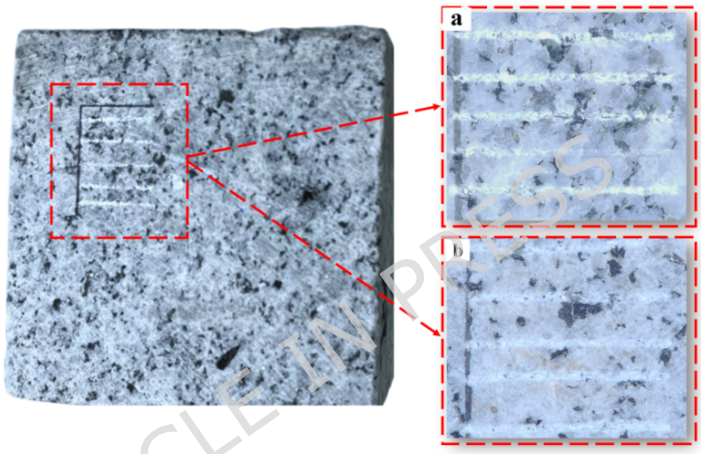

Fig. 12 Granite scratches at 100℃(a) and 400°C(b)

Different scratch behavior of granite after natural cooling by heat treatment at 100°C and 400°C

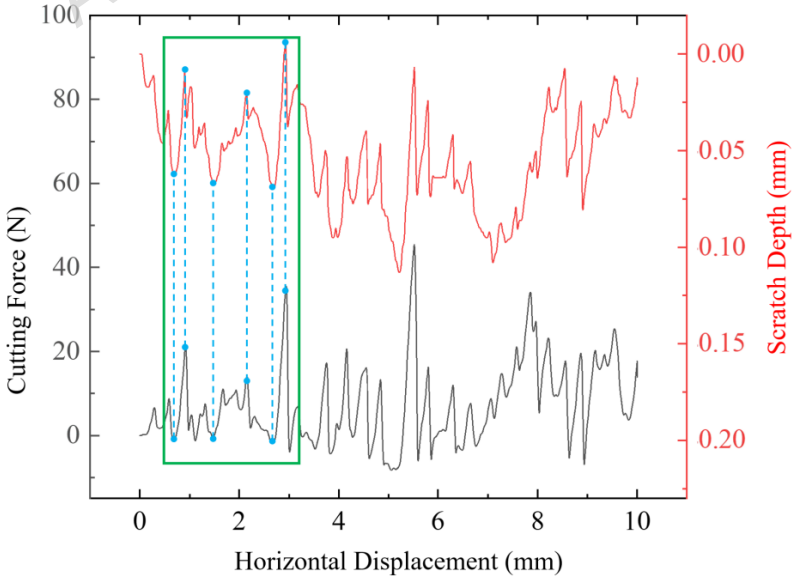

Fig. 13 Graph of cutting force and scratch depth variation with horizontal displacement

As the horizontal displacement of the probe increases, the cutting force and scratch depth show similar characteristics.